

Effect of Animal Orientation on Acoustic Estimates of Zooplankton Properties

Joseph D. Warren, Timothy K. Stanton, Duncan E. McGehee, and Dezhang Chu

Abstract—It is well known that the behavior of zooplankton and, in particular, their orientation distribution dramatically affects the level of backscattered acoustic energy. As a result, interpretation of acoustic survey data in the ocean is subject to error. In order to quantify these effects, laboratory data from two important classes of animals were collected. The data involved broad-band (350–650 kHz) acoustic signals insonifying individual animals whose orientation was varied over the range 0° – 360° in 1° increments. The animals were from two major anatomical groups: fluid-like (decapod shrimp; *Palaemonetes vulgaris*) and elastic-shelled (periwinkles; *Littorina littorea*). The data were analyzed both in the time domain (with pulse compression processing) and the frequency domain. Averages of the laboratory data over different orientation distributions illustrate the variability in average target strength that can be expected in the ocean environment. The average target strength of the shrimp varied by 3 dB when averaged over orientation distributions centered around broadside and end-on incidence. In addition, size estimates from pulse compression processing of the broad-band echoes were made for various orientation distributions for both the shrimp and periwinkles. These results show the necessity of animal orientation information for the proper interpretation of acoustic backscatter data.

Index Terms—Acoustic scattering, animal orientation, zooplankton.

I. INTRODUCTION

MEASUREMENTS of acoustic scattering in the ocean are used by biologists to determine the abundance of zooplankton in the water column [1]–[4]. However, there generally is not a simple relationship between the amount of sound scattered and the number and type of animals. Originally, the fluid sphere scattering model by Anderson [5] was used to model zooplankton. This spherical model was used by scientists to estimate animal biomass in the ocean and also to obtain information about the size distribution of the animals [1], [6], [7]. Research has shown that the simple model of a sphere is inadequate for modeling some types of zooplankton and that the orientation of the animal can have a profound effect on the scattering [8]–[11]. In an attempt to solve this problem, scientists have developed

more realistic models of the scattering physics for several types of zooplankton (see reviews in [7], [12]).

Although significant progress has been made on the development of scattering models, much still needs to be done. For example, a crucial element in understanding the scattering is its dependence upon the angle of orientation of the animal. The average level of scattering for some orientations can be predicted using available theory [13]. For other orientations, the models must be advanced in order to make reliable predictions. Given the fact that the models may be valid only for a certain range of orientations, a scattering analysis may involve supplementary laboratory data for animal orientations which the models do not accurately describe.

This paper describes a study where laboratory data involving two types of zooplankton were collected at high angular resolution and over an octave bandwidth. The data are processed in order to predict the effects of animal orientation on the scattering levels and on acoustic estimates of animal size. All laboratory data involve scattering by individual animals. For acoustic estimates of size in the ocean application, the animals must also be resolved acoustically. However, the study involving the effects of orientation on scattering levels applies to either case of resolved animals or echoes from an aggregation since the analysis involves echo energy and first-order scattering (higher order scattering is negligible for objects of such small target strength).

II. THEORY

Acoustic backscatter from a zooplankter is determined by the differences in density and sound speed between the animal and the surrounding fluid, the animal's shape, and the animal's size relative to the acoustic wavelength. By using simple geometric shapes to represent the animal, mathematical scattering models for several different types of zooplankton have been developed [14]. This paper discusses two types of zooplankton that have very different physical attributes and are thus modeled separately: those with fluid-like bodies and elastic-shelled animals.

Both of these animals have been successfully modeled with ray-based methods [13], [14]. These methods are an approximation to the scattering and are valid only in the geometrical scattering region ($ka > 1$), where k is the acoustic wavenumber and a is a characteristic dimension of the animal, generally its radius. In this study, ka ranges from 3 to 8. Acoustic rays are used to represent scattering from specific features or involving certain mechanisms of the scatterer. The advantage of this approach is that accurate representations of the scattering from an animal can be made by using the contributions from the most dominant mechanisms, while the disadvantage is that these results are only applicable in the geometric scattering region.

Manuscript received March 15, 2000; revised August 15, 2001. This work was supported in part by the Office of Naval Research under Grant N00014-96-1-0878 and Grant N00014-95-1-0287 and in part by the Woods Hole Oceanographic Institution (WHOI) Education Office under contribution 10198.

J. D. Warren, T. K. Stanton, and D. Chu are with the Applied Ocean Physics and Engineering Department of the Woods Hole Oceanographic Institution, Woods Hole, MA 02543 USA (e-mail: jwarren@whoi.edu).

D. E. McGehee was with the Applied Ocean Physics and Engineering Department of the Woods Hole Oceanographic Institution, Woods Hole, MA 02543 USA. He is now with BAE Systems, San Diego, CA 92123 USA.

Publisher Item Identifier S 0364-9059(02)00652-0.

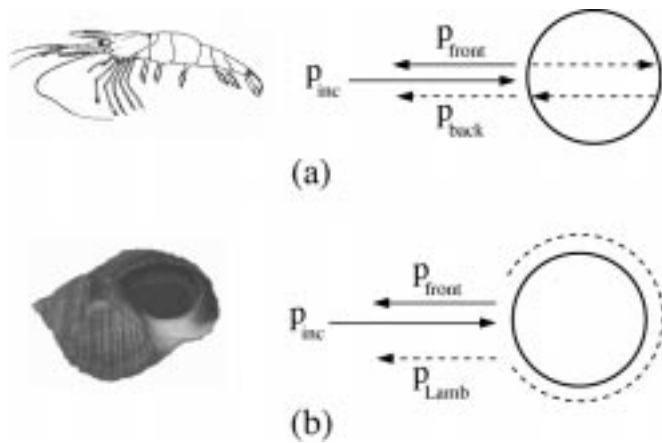


Fig. 1. Schematic drawing of certain scattering mechanisms for the (a) shrimp and (b) snail. p_{front} , p_{Lamb} and p_{back} are the pressure fields from the front interface reflection, the Lamb wave, and reflection off the back interface of the animal, respectively.

Common to both types of animals is the fact that an echo due to a single insonification of an individual animal will have multiple returns that can overlap in the time domain. The different returns are due to the various features of each animal that scatter sound. The overlap is due to the small size of the animals relative to the long pulse length of the acoustic wave that strikes the animal. With sufficiently high bandwidth in the insonifying signal and matched filter signal processing, some of the individual echoes by the features can be resolved. Otherwise, one would be measuring the constructive or destructive interference pattern from the overlapping echoes, which makes the analysis more of a challenge.

A. Fluid-Like Animals

Zooplankton whose body composition are fluid-like occur throughout the oceans. Common types of fluid-like animals include krill, amphipods, and decapod shrimp. These animals all have a morphology roughly similar to the species (*Palaemonetes vulgaris*) studied herein.

The class of fluid-like animals that *Palaemonetes vulgaris* belongs to has a very thin outer shell or exoskeleton (which is assumed not to support a detectable shear wave) enclosing the body of the animal which has physical characteristics that are similar, but not necessarily the same, as those of the surrounding medium. There is strong evidence that the scattering from the above-mentioned animals occurs primarily from reflections from the outer boundary of the animal. For example, previous studies involving krill and shrimp [15], [16] have found that near broadside incidence there are generally two main echoes from the animal: one from the front interface of the body, and a second echo from a wave that propagates through the animal's body, reflects off the interface at the far side of the animal, propagates back through the animal's body, and finally is detected by the receiver [Fig. 1(a)].

For the simple case of broadside incidence, the time delay between the arrivals of the two echoes provides useful information. The time delay will be directly proportional to the distance the wave travels inside the animal. Thus, the animal's diameter can be estimated if the speed of sound in the interior of

the animal is assumed to be constant. The ratio of sound speed of a fluid-like animal relative to that of the surrounding medium ($h = (c_{animal}/c_{seawater}) = 1.0279$) measured by Foote [17] for a euphausiid (a morphologically similar animal) is used. The animal's orientation relative to the acoustic wave will also affect the time delay. If the animal is at broadside incidence to the acoustic wave then the time delay can be converted directly to an estimate of the diameter of the animal. At oblique angles, the conversion of time-delay information to diameter estimates requires knowledge of the orientation and the use of simple trigonometry. This method is not applicable at all angles due to limitations of the scattering model near end-on incidence and is further complicated by the presence sometimes of more than two echoes [14]. These echoes are likely to occur from reflections from parts of the animal other than the front and back interface (such as the rostrum or telson).

B. Elastic-Shelled Animals

Periwinkles (*Littorina littorea*) are bottom-dwelling snails that are commonly found in intertidal zones. They are similar in morphology to certain planktonic pteropods (e.g., *Limacina retroversa*) which can be important acoustic scatterers in the water column [18]–[20]. The pteropods are very difficult to study individually in the laboratory due to their small size (diameters are generally less than 1 mm). Since there is strong evidence that periwinkles and planktonic snails have similar scattering characteristics [21], periwinkles were used in this study.

Scattering from elastic-shelled animals is characterized by a very strong echo specularly reflected by their hard shell. A previous study [21] has found that strong secondary echoes are also present. The secondary echoes have been determined to be from two different mechanisms: 1) a Lamb wave that travels along the animal's shell, partially circumnavigating the animal, and then returning in the backscatter direction [Fig. 1(b)] and 2) echoes from within the opercular opening. When the opening faces the transducer, the acoustic wave can travel inside the opening, scatter off the back wall, and return to the transducer. Scattering from the animal tissue itself is very weak relative to that from the shell since the animal tissue has a density and, presumably, a sound speed close to that of sea water. Therefore, the effect of the animal will be ignored and only scattering from the shell will be considered.

The scattered energy from the periwinkle has been shown to vary greatly with the orientation of the shell [21], due to the complexity of the shape of the animal's shell. Although somewhat cone-shaped, the shell is actually a tube that is coiled upon itself. Therefore, the thickness and surface roughness of the shell is variable. In fact, depending on the orientation of the animal, the number of echoes that are reflected differ due to the change in scattering characteristics. For example, when the opercular opening of the animal is facing away from the acoustic transmitter, there is no Lamb wave detected. This may be the result of all Lamb waves at that orientation being severely attenuated due to interaction with the opening.

It is possible to infer information on the properties of the elastic-shelled animal from the arrival times of the different waves that scatter from the animals. If the secondary arrival

corresponds to a Lamb wave, then the time delay between the echo from the front interface and the Lamb wave echo corresponds to the circumference of the animal (and thus its diameter) [Fig. 1(b)]. It should be noted that the second arriving ray in our two-ray model is referred to as the Lamb wave ray. This is somewhat misleading since a Lamb wave can only propagate along an elastic surface, not in the water. The Lamb wave ray referred to in this paper corresponds to the process of the portion of the incident field that initially travels through the water at a speed c , strikes the elastic shell and is coupled into a Lamb wave which propagates at c_{Lamb} , circumnavigates the shell, and “launches” back into the water where the wave is then detected by the receiver.

There are complicating factors in using the Lamb wave to infer properties of the target: the dispersive nature of the speed of the Lamb wave, the variable distance the Lamb wave travels along the shell, and the arrival of other Lamb waves that have circumnavigated the shell more than once. Lamb wave speeds for these frequencies and shell dimensions ($ka \sim 4-8$) have been observed and calculated to be subsonic, however, there have not been any direct measurements of their speed in calcium carbonate shells. Previous work [21] has estimated their average velocity as approximately one third of the speed of sound in sea water. While there is a dispersive relationship in Lamb wave velocities [23], [14], an average value will be used in this analysis while the statistical variability of the echo is explored for a single-sized animal and narrow range of frequencies.

The Lamb waves of interest do not travel a complete circumnavigation around the shell. There is a specific angle (θ_{Lamb}) relative to the axis of the shell where the wave starts or “lands” on the shell, as well as leaves or “launches” from the shell and returns to the water. Therefore, the arc traveled by the Lamb wave on a spherical shell is $2 \cdot (180^\circ - \theta_{\text{Lamb}})$. For subsonic waves, $\theta_{\text{Lamb}} = 90^\circ$ [23]. Lamb waves that have circumnavigated the shell multiple times will be delayed in time by approximately $(2\pi r)/(c_{\text{Lamb}})$ for each circumnavigation, where r is the radius of the shell (0.003 m) and $c_{\text{Lamb}} = 500$ m/s. Therefore, the expected time delay between multiple-circumnavigating Lamb waves is $\sim 38 \mu\text{s}$, which is less than our pulse length of $200 \mu\text{s}$. Returns from multiple circumnavigations of the Lamb wave should be detected under the conditions discussed above, however, our analysis will only use the first two waves that are detected (the specular reflection and the first Lamb wave). Finally, it should be noted that although subsonic Lamb waves for idealized spherical shells have been calculated under certain conditions to have a low-quality factor which should pose a challenge in resolving such waves [23]; they are, indeed, resolvable in these studies involving the irregularly shelled objects.

C. Pulse Compression Processing

Pulse compression (PC) processing is a signal processing technique that has recently been used to analyze backscattered echoes from biological targets [15], [16]. It is similar to a matched filter which has been used in radar and sonar analysis for quite some time [24]. PC processing involves the cross correlation of the received scattered signal with the calibration signal. When the scatterer has a uniform frequency response,

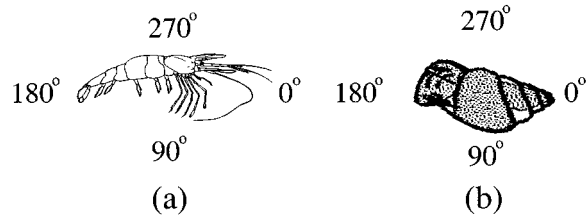


Fig. 2. Orientation of incident acoustic wave relative to the: (a) shrimp and (b) snail. 0° incidence is approximately “head-on” and “apex-on” incidence for the two animals, respectively.

PC processing is identical to a matched filter and its output is a single main lobe with small sidelobes. Deviations from this pattern provide information on the scattering characteristics of the target. For example, the presence of two large lobes may correspond to two major scattering features on the target.

III. EXPERIMENTAL METHODS

The experimental procedures used in this study have been described previously [16], [21], [25], [26]); therefore, only a brief summary will be presented. An array of 16 pairs of transducers configured in a bistatic arrangement and aimed in the horizontal direction was placed in a large fiberglass tank filled with sea water. For the data presented herein, a “chirp” signal, centered at 500 kHz, was generated with a bandwidth of approximately 300 kHz. The pulse length was $200 \mu\text{s}$. After the acoustic wave scattered off the animal, the echo in the backscatter direction was detected by a receiving transducer, identical and adjacent to the transmitting one. After amplification, the received signal was digitized and displayed on a digital oscilloscope, and then transferred to a computer for analysis. For each experiment, an individual animal was suspended with a thin monofilament line ($59\text{-}\mu\text{m}$ diameter) that was acoustically transparent. A single line was used for the periwinkle shell, while a two-line configuration was used with the live shrimp. The two-line “harness” restricted the shrimp’s movement and permitted better control of its orientation. The top of each tether was attached to the axis of a stepper motor which was used to rotate the animal.

The decapod shrimp was tied such that the animal was to within about 20° of lying flat on its side in the horizontal plane. The shrimp was rotated in this plane so that scattering information in the dorsal/ventral aspect was obtained (Fig. 2). The periwinkle was tied such that it could be rotated for apex/opercular opening scattering. The planes of rotation were selected so as to provide animal orientations that may be found in the field. The decapod shrimp remained alive during the experiment, and the periwinkle experiment involved scattering from the shell only since the periwinkle tissue has acoustical properties very close to that of the surrounding water. The tissue was removed beforehand being replaced with water for convenience, as the scattering characteristics with tissue or water are not expected to change significantly. Great care was taken to prevent accumulation of bubbles onto the tether and bodies of the animals.

Postprocessing of the data involved the use of a digital bandpass filter (to remove noise) and then PC processing. The compressed echoes were then processed through use of an automatic peak detection algorithm to determine the time of arrival and

TABLE I

DIMENSIONS OF THE ANIMALS USED IN THE EXPERIMENT. LENGTH OF THE SHRIMP MEASURED BETWEEN ANTERIOR OF THE EYE AND END OF THE TELSON. DIAMETER OF THE SHRIMP IS THE AVERAGE OF THE MEASUREMENT FOR EACH OF THE FIRST TWO THORACIC SEGMENTS. LENGTH OF THE PERIWINKLE IS THE MAXIMUM TIP-TO-TIP DISTANCE. DIAMETER OF THE PERIWINKLE WAS MEASURED BETWEEN THE PLANE CONTAINING THE FACE OF THE OPERCULAR OPENING AND THE OUTER POINT OF THE SHELL ON THE OPPOSITE SIDE OF THE SHELL

Common Name	Species	Length	Diameter
Grass Shrimp (#06)	<i>Palaemonetes vulgaris</i>	19.37 mm	4.15 mm
Periwinkle (#01)	<i>Littorina littorea</i>	6.2 mm	3.9 mm

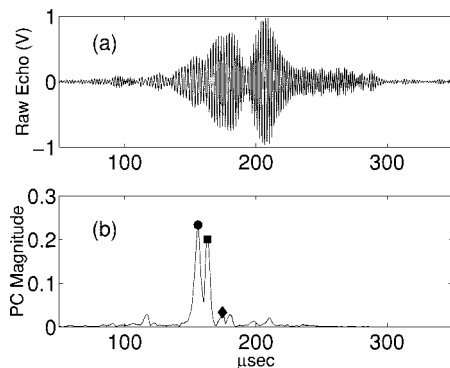


Fig. 3. Example echo from decapod shrimp: (a) raw echo voltage (b) envelope of pulse compression output showing the primary (○), secondary (□) and tertiary (◇) returns.

magnitude of the individual scattered rays. The largest and generally earliest occurring echo is referred to as the primary peak, and the remaining peaks are ordered by their arrival time (secondary, tertiary).

IV. RESULTS

A. Fluid-Like Animal

A total of ten decapod shrimp were used in the experiment with echoes collected at 1° increments over two complete rotations (720°) of the shrimp's body. Results were similar for all animals, so only results from one animal (#6) are presented herein (Table I). The raw echo (before PC processing) is difficult to interpret since it is composed of overlapping echoes from at least two reflections from the animal [Fig. 3(a)], however, the PC output clearly distinguishes several distinct echo arrivals from the animal [Fig. 3(b)]. The magnitude of the primary and secondary arrivals (as well as the raw echo level) vary regularly with angle of orientation (Fig. 4). The peaks of the echo levels correspond to when the shrimp is at broadside incidence ($\theta = 90^\circ, 270^\circ, 450^\circ, 630^\circ$) to the insonifying wave.

Information about the animal can be extracted from the timing of the PC echo arrivals. Estimates of the animal's dimension were made from the time delay between the primary and secondary echo arrivals for all angles of orientation (Fig. 5). These estimates assume a uniform sound speed for the inside of the animal's body. The mode of this distribution is 4.2 mm

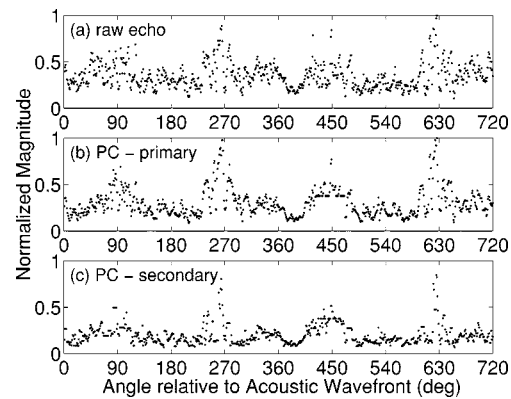


Fig. 4. Normalized magnitude of: (a) raw echo voltage, (b) primary, and (c) secondary peaks of PC output for shrimp #6. Odd multiples of 90° correspond to broadside incidence, while even multiples of 90° correspond to end-on incidence. Magnitudes of the secondary peaks are normalized to the largest overall value of the primary return.

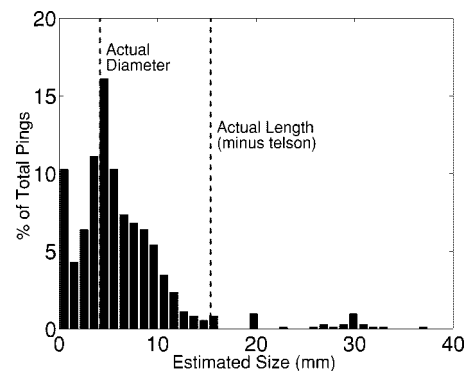


Fig. 5. Histogram of uncorrected estimated diameter of shrimp #6 for pings from all angles of orientation ($0-720^\circ$). Mode of distribution is 4.2 mm. Measured diameter was 4.15 mm.

which agrees very well with the measured animal diameter of 4.15 mm at the widest section. However, there are estimates of the animal's size that are smaller than the animal's dimensions. It is possible that they are associated with reflections from the narrower or tapered part of the animal's cephalothorax and telson. There are several outlying estimates of the animal's dimension that are larger than the physical length of the animal (19.37 mm). These may be due to noise or artifacts of the PC processing. However, the main "body" of the histogram ends at approximately 15 mm which is a reasonable estimate of the length of the animal if the telson (which is quite thin) is excluded. These results suggest that a single animal insonified by multiple pings can be sized using information from multiple features of the compressed echo from the animal.

An important aspect of this analysis is to use the laboratory data to estimate the variability that one might expect in measurements in the ocean. One source of variability is the dependence of the scattering upon orientation coupled with the variability in orientation of the animals. Since the laboratory data involved measurements of scattering for all angles of orientation (in one plane) and in small increments, the data can be used, along with information on distributions of animal orientation, to estimate the variability. The pulse compression analysis involves using

TABLE II

ACOUSTIC ESTIMATES OF ANIMAL DIAMETER FOR DIFFERENT ASSUMED ANIMAL ORIENTATION DISTRIBUTIONS. THE CALCULATIONS INVOLVE USE OF THE LABORATORY DATA. ALL SIZES ARE IN MILLIMETERS. UNCORRECTED DIAMETERS ARE CALCULATED FROM TIME DELAYS BETWEEN PRIMARY AND SECONDARY ARRIVALS. FOR THE SHRIMP, A CORRECTED DIAMETER WAS DETERMINED BY TAKING INTO ACCOUNT THE KNOWN ORIENTATION IN THE ESTIMATION OF THE DIAMETER. ANIMAL SIZE FOR THE SHRIMP IS THE MEASURED DIAMETER AND FOR THE PERIWINKLE IT IS THE AVERAGE OF THE MEASURED LENGTH AND DIAMETER OF THE SHELL. THERE IS NO DIAMETER ESTIMATE FOR THE PERIWINKLE IN THE BACK-OF-SHELL CASE DUE TO THE ABSENCE OF A DETECTABLE LAMB WAVE. THERE IS NO CORRECTED DIAMETER FOR THE SHRIMP AT END-ON INCIDENCE SINCE THE TRIGONOMETRIC MODEL IS NOT APPLICABLE AT THOSE ANGLES

Animal	Orientation Distribution θ	Estimated Diam. (no correction)		Estimated Diam. (with correction)		Anim. Size
		Mean	Mode	Mean	Mode	
		Shrimp	Down-Looking Sonar $290^\circ \pm 20^\circ$	4.9	3.7	
Shrimp	Uniform 1 – 360°	6.0	4.2	4.2	3.0	4.15
Shrimp	Broadside Incidence $90^\circ \pm 20^\circ$, $270^\circ \pm 20^\circ$	4.2	4.3	4.1	4.3	4.15
Shrimp	End-On Incidence $0^\circ \pm 20^\circ$, $180^\circ \pm 20^\circ$	6.2	5.1	NA	NA	4.15
Periwinkle	Down-Looking Sonar $250^\circ \pm 40^\circ$	5.2	6.0	NA	NA	5.1
Periwinkle	Uniform 1 – 360°	5.6	4.1	NA	NA	5.1
Periwinkle	Apex Incident $20^\circ \pm 10^\circ$	4.6	4.4	NA	NA	5.1
Periwinkle	Opercular Incident $270^\circ \pm 10^\circ$	5.0	5.9	NA	NA	5.1
Periwinkle	Back of Shell Inc. $180^\circ \pm 10^\circ$	NA	NA	NA	NA	5.1

data from resolved animals in the laboratory to estimate the variability from resolved animals in the ocean. The target strength analysis, which involves a form of echo energy, could involve either single targets in the ocean or averaged echoes from multiple targets. An assumption in the latter case is that the orientation distribution of each animal is the same. The majority of sonars used in zooplankton surveys are downward looking. The echoes from these sonars would insonify shrimp from the dorsal/ventral plane rather than the left-/right-side plane that a side-looking sonar would encounter.

There is no definitive work on the orientation of decapod shrimp or euphausiids in the ocean. Sameoto [27] studied the orientation of euphausiids in the water column from photographs taken from a net system. There was generally a broad range of orientations for the animals, however, at certain times (1500 h and 2400 h), his results show a preferred orientation of the animal being slightly head-up in the water column, relative to an otherwise horizontal orientation. Also, several other studies [28], [29] show that krill exhibit this head-up position for certain behaviors. We use this orientation distribution as a basis for our modeling of what a downward-looking sonar would detect. Since it is likely that animal orientation distributions change throughout the day depending upon the

behavior of the animal (vertical migration and feeding for example), other ranges of orientations are studied. Multiple scattering effects are ignored in this case since zooplankton are weak scatterers. Size estimates (Table II) and target strength values (Table III) were calculated for the various synthetic data sets (“synthetic” in that the laboratory data were used for the calculations in combination with the various orientations expected in the ocean environment).

The calculations involving different orientation distributions show that there are changes in the mean value and variance of what would be the ocean-measured target strength of the animal (Table III). Although the variances in the target strength for a given orientation distribution are substantial (due to the wide frequency range used and the frequency dependence of the scattering), there are also changes in the mean target strength between the various orientation distributions. The differences are largest (~ 3 dB) between the distributions centered around end-on and broadside incidence. While these differences are smaller than those observed at lower frequencies [11], they are large enough to cause substantial changes in biomass estimates. Given the importance of biomass estimates, these calculations indicate the need for more information on *in situ* animal orientation.

TABLE III
TARGET STRENGTH STATISTICS FOR DIFFERENT ASSUMED ORIENTATION DISTRIBUTIONS. THE CALCULATIONS INVOLVED USE OF THE LABORATORY DATA

Animal	Orientation Distribution (θ)	$\overline{TS} \pm \sigma_{TS}^2$ 350-650 kHz
Shrimp	Down-Looking ($290^\circ \pm 20^\circ$)	-91.1 ± 2.8
Shrimp	Uniform ($1 - 360^\circ$)	-90.5 ± 6.4
Shrimp	Broadside ($90^\circ \pm 20^\circ, 270^\circ \pm 20^\circ$)	-88.5 ± 9.8
Shrimp	End-On ($0^\circ \pm 20^\circ, 180^\circ \pm 20^\circ$)	-91.7 ± 4.7
Periwinkle	Down-Looking ($250^\circ \pm 40^\circ$)	-57.8 ± 1.3
Periwinkle	Uniform ($1 - 360^\circ$)	-57.7 ± 8.6
Periwinkle	Apex ($20^\circ \pm 10^\circ$)	-63.8 ± 2.6
Periwinkle	Opercular ($270^\circ \pm 10^\circ$)	-57.0 ± 0.8
Periwinkle	Back of Shell ($180^\circ \pm 10^\circ$)	-53.8 ± 4.3

The calculations using the laboratory data were also used to determine how changes in animal behavior in the ocean may change estimates (using data from ocean measurements) of the animal's size from time-delay measurements from the PC processing (Table II). An "uncorrected" diameter estimate (d') was found by converting the time delay between the primary and secondary peaks in the pulse compressed echo (τ) to a length without using any orientation information

$$d' = \frac{\tau c_{\text{animal}}}{2}, \quad (1)$$

A "corrected" animal diameter (d) was calculated taking into account orientation using a simple trigonometric relationship

$$d = d' \sin \theta \quad (2)$$

where θ is the angle of the animal relative to the acoustic wavefront as shown in Fig. 2. The mean and mode of the corrected and uncorrected diameter estimates for the various orientations were found. For the uncorrected estimates of diameter, the mode of the distribution had a better agreement with the measured diameter of the shrimp, however when geometric information was included to correct the estimate, the mean value was closer to the measured diameter. In the case of broadside incidence, the acoustic estimates of diameter and the measured value agreed almost exactly, for the other animal behaviors the acoustic estimates tended to overestimate the measured value. There was no calculation of estimated diameter for the end-on incidence case since the theoretical model used is not applicable at those angles.

To examine the accuracy of the theoretical two-ray model and the orientation corrections to the diameter estimates, a comparison of uncorrected diameters, corrected diameters, and theoretically predicted uncorrected diameters was made (Fig. 6). For a range of angles from head-on (0°) to end-on (180°) incidence with 1° increments, mean time delays were calculated and then converted to uncorrected diameter estimates. These values were then corrected using the orientation of the animal and (2). Using

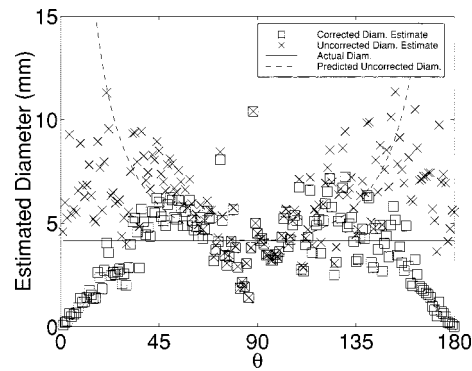


Fig. 6. Uncorrected (\times) and corrected (\square) diameter estimates of the shrimp from the time delay between primary and secondary PC peaks. For each 1° increment, four data points from two complete revolutions of the animal ($0-720^\circ$) were averaged to provide a data set covering 180° from head-on to end-on incidence. For example, the data point at 30° is the mean of the values collected at $30^\circ, 330^\circ, 390^\circ,$ and 690° . The dashed line is a theoretical prediction of the uncorrected diameter estimate using the measured animal diameter of 4.15 mm. The corrected and uncorrected scattering model appear to produce reasonable estimates within the range of $\pm 50^\circ$ and $\pm 35^\circ$, respectively, from broadside incidence.

the measured value of the animal's diameter, a theoretical prediction for the uncorrected diameter is made with the formula similar to (1):

$$d'_{\text{theoretical}} = \frac{d_{\text{measured}}}{\sin \theta}. \quad (3)$$

Obviously this equation is not valid for orientations near end- or head-on incidence since the diameter prediction goes to infinity. A comparison of the two estimates of diameter and the measured value shows that the valid range of orientations for the corrected and uncorrected estimates are approximately $\pm 50^\circ$ and $\pm 35^\circ$, respectively, relative to broadside incidence. The uncorrected estimates follow the theoretical trend for uncorrected data within about $\pm 60^\circ$ from broadside incidence.

B. Elastic-Shelled Animal

Six periwinkle shells (*Littorina littorea*) were used in the experiment. Since results were similar for all cases, those corresponding only to animal #1 are shown (Table I). Similar to the decapod shrimp analysis, individual ray echoes are difficult to identify in the raw echo, but are clearly shown in the PC processed echo (Fig. 7). The interference between the reflection from the front interface and the other echoes can change the overall amplitude of the received total echo. The major structure in the polar plots of echo versus orientation for the raw echo voltage and the primary peak magnitude are broadly similar (Fig. 8). There are differences in the smaller scale structure between the two plots which indicate the interference effect of the secondary echo. These secondary echoes are readily apparent in the PC processed signal and can provide information about the size of the animal.

For certain orientations, the time delay between the primary and secondary peak corresponds to the time difference between the echo from the front interface and a circumnavigating Lamb wave that travels subsonically around the shell and then couples, or launches, from the shell into the water [21]. At these values of

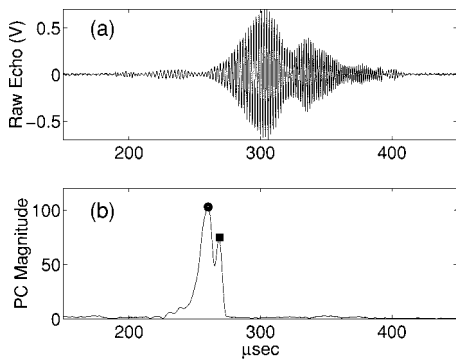


Fig. 7. Example echo from periwinkle. (a) Raw echo voltage. (b) Envelope of pulse compression output showing the primary (○) and secondary (□) returns.

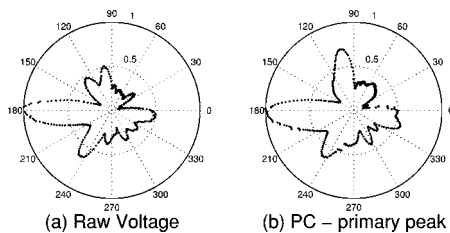


Fig. 8. Polar plot of scattering by a periwinkle versus angle of orientation. (a) Normalized raw echo amplitude. (b) Normalized primary PC peak.

ka , the Lamb wave speed that was both calculated and gave the best fit to the data in [21] involving the strongest subsonic secondary waves was approximately $c_{\text{Lamb}} = 500$ m/s. Although Lamb wave speeds are frequency-dependent, this average value can provide useful information. The term “Lamb wave speed” refers only to the speed that the Lamb wave propagates along the shell; when the “Lamb wave” ray is in the water column it travels at the speed c . Using this speed, the size of the periwinkle studied can be inferred from the acoustic data. If the shell is assumed to be circular, the diameter, d , of the shell can be found from the formula

$$d = \frac{\tau}{\left(\frac{1}{c} + \frac{\pi}{2c_{\text{Lamb}}}\right)} \quad (4)$$

where τ is the time delay between primary and secondary pulse compressed echo arrivals, and the distance traveled by the Lamb wave is halfway around the shell [23].

There is a fair amount of variation in the time delay between the primary and secondary peaks from the periwinkle (Fig. 9), which could be explained by Lamb wave speeds varying due to changes in shell thickness [21] or, since the shell is not circular, that the path length (and travel time) of the Lamb wave will vary depending on the orientation of the shell. However, there is a sharp peak in the distribution at $18.5 \mu\text{sec}$. Using (4), the estimated diameter of the shell is found to be 4.8 mm (compared to the measured diameter and length of 3.9 mm and 6.2 mm, respectively). Since the shell is not circular, it is reasonable to calculate the average of the diameter and length and use this value of 5.1 mm as the size of the periwinkle. Thus, the average size of the animal can be estimated using a two-ray model for the scattering and PC processing to resolve the multiple returns.

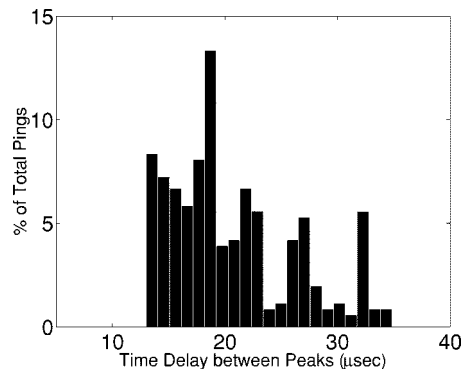


Fig. 9. Histogram of time delay between primary and secondary PC peaks of the periwinkle. Mode of distribution is $18.5 \mu\text{s}$, which corresponds to an estimated diameter of 4.8 mm. The mean of the measured diameter and length of the shell is 5.1 mm. There is a threshold of $13 \mu\text{s}$ in the peak detection algorithm.

As was done for the shrimp, synthetic data sets were created from the laboratory data to model data that might be collected using different sonar viewing angles in the ocean. Planktonic pteropods have been observed to have a preferred orientation in the water column. For both feeding and swimming, these animals position themselves with their opercular opening pointing mostly vertically upward [30], [31]. Therefore, with a downward-looking sonar, the opercular opening would be generally aimed toward the transducer and the apex would be aimed downward and to the side. In addition to the down-looking sonar data set, synthetic data sets were created for a uniform distribution, apex-upward, opercular opening-upward and back of shell-upward distributions. These different data sets show how the resulting size estimates (Table II) and target strengths (Table III) can change with various animal orientations in the ocean.

It is apparent given the range in target strength values (~ 10 dB) that large errors in estimates of animal populations can occur if the wrong orientation distribution were used in modeling these animals. However, all of the various distributions provide a similar range of estimates for the size of the animal. This indicates that the Lamb wave speed and path are relatively stable across the range of orientations, at least when averaged over the distance traveled around the shell.

Given that the scattering mechanism for the elastic-shelled animal is affected by the complex shape of the animal, a simple model that does not take into account the actual geometry of these shells will not provide a realistic representation of the scattering from these animals. However, a simple ray model may offer a reasonable approximation for describing the broad trends in how animal orientation can affect the backscattered energy.

V. DISCUSSION

This study has shown that, for this method of broad-band insonification in the geometric scattering region, the following is true.

- 1) For the elastic-shelled animal, acoustic estimates of size using pulse compression processing were accurate for *all* distributions of orientation studied, in spite of the fact that the target strength varied by 10 dB over the same distributions.

- 2) For the fluid-like animal, accurate acoustic estimates of size using pulse compression processing and the simple two-ray model require that the animal's *in situ* orientation distribution be to within about 35° of broadside incidence.
- 3) The fluid-like animal had a change of 3 dB in target strength averaged over a wide frequency band for different orientation distributions.

Acoustic scattering models are vital to understanding and interpreting measurements of biological scattering in the ocean. However, these models depend upon a variety of parameters which are often unknown, such as the animal's size and orientation distribution. This study presents results that show how different animal orientations could impact measurements of target strength and scattering-model-based estimates of animal size for two types of zooplankton (fluid-like and elastic-shelled).

Target strength measurements at these high frequencies show a range of values for the different orientation distributions for both types of zooplankton. Changes were smaller for the fluid-like animals, but still quite substantial (a 3-dB difference corresponds to a factor of two change in biomass estimates). Differences for the elastic-shelled animal were even larger.

Size estimates of single animals can be made with the use of pulse compression processing. In spite of the large variability of target strength for various orientations for elastic-shelled animals, the different orientation distributions caused only small changes in the acoustic estimates of size. With the ray model used, orientation information may not be needed for accurate size estimates of the elastic-shelled animals, although note that the dispersive properties of the Lamb waves for this irregular target need to be better understood for practical sizing methods in the ocean. Also, for fluid-like animals, acoustic estimates of size were not accurate unless the orientations were within about 35° of broadside incidence.

Target strengths and size estimates show a possibility for being used to categorize different animal behaviors. This method seems particularly suited to fluid-like animals where studies have shown the strong effect that animal orientation has on scattering spectra. Since animal behavior (and the orientation distribution) will change throughout the day, more studies of animal *in situ* orientation are needed if acoustic scattering models are to be used correctly and effectively.

REFERENCES

- [1] D. V. Holliday, R. E. Pieper, and G. S. Kleppel, "Determination of zooplankton size and distribution with multifrequency acoustic technology," *J. Cons. Int. Explor. Mer.*, vol. 46, pp. 52–61, 1989.
- [2] S. L. Smith, R. E. Pieper, M. V. Moore, L. G. Rudstam, C. H. Greene, J. E. Zamon, C. N. Flagg, and C. E. Williamson, "Acoustic techniques for the *in situ* observation of zooplankton," *Arch. Hydrobiol. Beih.*, vol. 36, pp. 1–21, 1992.
- [3] A. S. Brierley and J. L. Watkins, "Acoustic targets at South Georgia and the South Orkney islands during a season of krill scarcity," *Marine Ecology Progress Series*, vol. 138, pp. 51–61, 1996.
- [4] P. H. Wiebe, D. G. Mountain, T. K. Stanton, C. H. Greene, G. Lough, S. Kaartvedt, J. Dawson, and N. Copley, "Acoustical study of the spatial distribution of plankton on Georges Bank and the relationship between volume backscattering strength and the taxonomic composition of the plankton," *Deep-Sea Res. II*, vol. 43, pp. 1971–2001, 1996.
- [5] V. C. Anderson, "Sound scattering from a fluid sphere," *J. Acoust. Soc. Amer.*, vol. 22, pp. 426–431, 1950.
- [6] C. F. Greenlaw, "Acoustical estimation of zooplankton populations," *Limnol. Oceanogr.*, vol. 24, pp. 226–242, 1979.
- [7] D. V. Holliday and R. E. Pieper, "Bioacoustical oceanography at high frequencies," *ICES J. Marine Sci.*, vol. 52, pp. 279–296, 1995.
- [8] C. F. Greenlaw, "Backscattering spectra of preserved zooplankton," *J. Acoust. Soc. Amer.*, vol. 62, pp. 44–52, 1977.
- [9] A. Kristensen and J. Dalen, "Acoustic estimation of size distribution and abundance of zooplankton," *J. Acoust. Soc. Amer.*, vol. 80, pp. 601–611, 1986.
- [10] T. K. Stanton, P. H. Wiebe, and D. Chu, "Differences between sound scattering by weakly scattering spheres and finite-length cylinders with applications to sound scattering by zooplankton," *J. Acoust. Soc. Amer.*, vol. 103, pp. 254–264, 1998.
- [11] D. E. McGehee, R. L. O'Driscoll, and L. V. Martin-Traykovski, "Effects of orientation on acoustic scattering from Antarctic krill at 120 kHz," *Deep-Sea Res. II*, vol. 45, pp. 1273–1294, 1998.
- [12] K. G. Foote and T. K. Stanton, "Acoustical methods," in *ICES Zooplankton Methodology Manual*, R. Harris, P. H. Wiebe, J. Lenz, H. R. Skjoldal, and M. Huntley, Eds, London, U.K.: Academic, 2000, ch. 6, pp. 223–258.
- [13] T. K. Stanton and D. Chu, "Review and recommendations for modeling of acoustic scattering by fluid-like elongated zooplankton: Euphausiids and copepods," *ICES J. Marine Sci.*, vol. 57, pp. 793–807, 2000.
- [14] T. K. Stanton, D. Chu, and P. H. Wiebe, "Sound scattering by several zooplankton groups. II. Scattering models," *J. Acoust. Soc. Amer.*, vol. 103, pp. 236–253, 1998.
- [15] D. Chu and T. K. Stanton, "Application of pulse compression techniques to broadband acoustic scattering by live individual zooplankton," *J. Acoust. Soc. Amer.*, vol. 104, pp. 39–55, 1998.
- [16] T. K. Stanton, D. Chu, P. H. Wiebe, L. V. Martin, and R. L. Eastwood, "Sound scattering by several zooplankton groups. I. Experimental determination of dominant scattering mechanisms," *J. Acoust. Soc. Amer.*, vol. 103, pp. 225–235, 1998.
- [17] K. G. Foote, I. Everson, J. L. Watkins, and D. G. Bone, "Target strengths of Antarctic krill (*Euphausia superba*) at 38 and 120 kHz," *J. Acoust. Soc. Amer.*, vol. 87, pp. 16–24, 1990.
- [18] T. K. Stanton, P. H. Wiebe, D. Chu, M. C. Benfield, L. Scanlon, L. Martin, and R. L. Eastwood, "On acoustic estimates of zooplankton biomass," *ICES J. Marine Sci.*, vol. 51, pp. 505–512, 1994.
- [19] M. C. Benfield, C. S. Davis, P. H. Wiebe, S. M. Gallagher, R. G. Lough, and N. J. Copley, "Video plankton recorder estimates of copepod, pteropod and larvacean distributions from a stratified region of Georges Bank with comparative measurements from a MOCNESS sampler," *Deep-Sea Res. II*, vol. 43, pp. 1925–1945, 1996.
- [20] P. H. Wiebe, T. K. Stanton, M. C. Benfield, D. G. Mountain, and C. H. Greene, "High-frequency acoustic volume backscattering in the Georges Bank coastal region and its interpretation using scattering models," *IEEE J. Oceanic Eng.*, vol. 22, pp. 445–464, 1997.
- [21] T. K. Stanton, D. Chu, P. H. Wiebe, R. L. Eastwood, and J. D. Warren, "Acoustic scattering by benthic and planktonic shelled animals," *J. Acoust. Soc. Amer.*, vol. 108, pp. 535–550, 2000.
- [22] S. G. Kargl and P. L. Marston, "Observations and modeling of the backscattering of short tone bursts from a spherical shell: Lamb wave echoes, glory, and axial reverberations," *J. Acoust. Soc. Amer.*, vol. 85, pp. 1014–1028, 1989.
- [23] L. G. Zhang, N. H. Sun, and P. L. Marston, "Midfrequency enhancement of the backscattering of tone bursts by thin spherical shells," *J. Acoust. Soc. Amer.*, vol. 91, pp. 1862–1874, 1992.
- [24] G. L. Turin, "An introduction to matched filters," *IRE Trans. Inform. Theory*, vol. IT-6, pp. 311–329, 1960.
- [25] T. K. Stanton, "Sound scattering by spherical and elongated shelled bodies," *J. Acoust. Soc. Amer.*, vol. 88, pp. 1619–1633, 1990.
- [26] D. Chu, T. K. Stanton, and P. H. Wiebe, "Frequency dependence of sound backscattering from live individual zooplankton," *ICES J. Marine Sci.*, vol. 49, pp. 97–106, 1992.
- [27] D. D. Sameoto, "Quantitative measurements of euphausiids using a 120-kHz sounder and their *in situ* orientation," *Can. J. Fisheries Aquatic Sci.*, vol. 37, pp. 693–702, 1980.
- [28] U. Kils, "The swimming behavior, swimming performance and energy balance of Antarctic krill, *Euphausia superba*," *BIOMASS Science Series*, vol. 3, 1981.
- [29] K. Miyashita, I. Aoki, and T. Inagaki, "Swimming behavior and target strength of isada krill (*Euphausia pacifica*)," *ICES J. Marine Sci.*, vol. 53, pp. 303–308, 1996.
- [30] J. E. Morton, "The biology of *Limacina retroversa*," *J. Mar. Biol. Ass. U.K.*, vol. 33, pp. 297–312, 1954.
- [31] R. W. Gilmer and G. R. Harbison, "Morphology and field behavior of pteropod molluscs: Feeding methods in the families cavoliniidae, limaciniidae and peraciliidae (gastropoda: Thecosomata)," *Marine Biol.*, vol. 91, pp. 47–57, 1986.



Joseph D. Warren received the B.S. degree in engineering from Harvey Mudd College, Claremont, CA, in 1994 and the Ph.D. degree in applied ocean sciences from the Massachusetts Institute of Technology/Woods Hole Oceanographic Institution Joint Program in Oceanography and Oceanographic Engineering, Woods Hole, MA, in 2000.

He is currently an Office of Naval Research Postdoctoral Fellow in Ocean Acoustics at the Woods Hole Oceanographic Institution and the Southwest Fisheries Science Center in La Jolla,

CA. His research interests include the use of high-frequency acoustics to map and identify distributions of zooplankton, acoustic scattering processes, and zooplankton ecology.

Dr. Warren is a member of the Acoustical Society of America, the American Geophysical Union, and the American Society of Limnology and Oceanography.



Timothy K. Stanton received the B.S. degree in physics from Oakland University, Rochester, MI, in 1974 and the M.S. and Ph.D. degrees in physics from Brown University, Providence, RI, in 1977, and 1978, respectively. His undergraduate research involved experiments in solid state acoustics with Dr. Norman Tepley as advisor and his graduate research involved nonlinear acoustics measurements and instrumentation development with Dr. Robert Beyer as advisor.

From 1978 to 1980, he was a Senior Engineer at the Submarine Signal Division of Raytheon Company, Portsmouth, RI, where he was engaged in research, development and testing of acoustic systems. From 1980 to 1988, he was a member of the scientific staff of the Department of Geology and Geophysics, University of Wisconsin-Madison, where he conducted various theoretical, laboratory, and field studies in acoustical oceanography with Dr. Clarence Clay. From 1988 to present, he has been a member of the scientific staff of the Department of Applied Ocean Physics and Engineering of the Woods Hole Oceanographic Institution (WHOI), Woods Hole, MA, and is currently Senior Scientist. He is currently working in collaboration with Dr. Peter Wiebe at WHOI and other colleagues in development of acoustic scattering models of marine organisms through various theoretical and laboratory methods and applying the methods to field surveys. In addition to his research, he is part of the Massachusetts Institute of Technology and WHOI Joint Graduate Education Program and teaches acoustic scattering theory. Overall, he has published papers covering the areas of nonlinear acoustics, acoustics instrumentation, fiber-optic hydrophones, and acoustic scattering by volumetric objects, seafloor, sea surface and underside of sea ice.

He has served as Associate Editor for the *Journal of the Acoustical Society of America* and as Guest Editor for *Deep Sea Research*. Dr. Stanton is a Fellow of the Acoustical Society of America and a member of The Oceanography Society. In 1985, he was awarded the A.B. Wood Medal for Distinguished Contributions to Underwater Acoustics. He has served as Guest Editor for a special issue of the IEEE JOURNAL OF OCEANIC ENGINEERING.



Duncan E. McGehee received the B.M.E. degree in mechanical engineering from the Georgia Institute of Technology, Atlanta, in 1982, the M.S. degree in mechanical engineering from the University of California at Berkeley in 1983, and the Ph.D. degree in electrical engineering from the University of California at San Diego in 1994. His graduate research involved the development of a three-dimensional acoustical imaging system for observations of zooplankton behavior.

From 1983 to 1987, he was a Mechanical Engineer at the Garrett Turbine Engine Company, Phoenix, AZ, where he designed and tested turbofan engines. From 1994 to 1996, he was a Post-Doctoral Scholar at the Woods Hole Oceanographic Institution, Woods Hole, MA, where he worked with the other authors measuring and modeling acoustic scattering from zooplankton. From 1996 to the present, he has worked at BAE SYSTEMS (formerly Tracor), in continuing studies of zooplankton acoustic scattering and their applications to deep- and shallow-water oceanic ecosystems. He is also developing acoustic methods for counting and tracking deep diving whales. His research interests include high-frequency acoustics, biological oceanography, behavioral ecology, acoustics of whales and dolphins, and the philosophy of science and technology. He has published papers in the areas of zooplankton acoustics, zooplankton behavior, biological oceanography, and advanced transducers and sonars.



Dezhang Chu received the B.A. degree in electrical engineering from China University of Geosciences, Wuhan, China, in 1982 and the Ph.D. degree in geophysics from the University of Wisconsin-Madison in 1989.

He was a Post-Doctoral Scholar at the Woods Hole Oceanographic Institution (WHOI), Woods Hole, MA, from 1989 to 1990 and a Post-Doctoral Investigator at WHOI from 1990 to 1991. He is currently a Research Specialist at WHOI in the Department of Applied Ocean Physics and

Engineering. His research interests include wave propagation and reverberation in shallow-water, acoustic scattering, and seafloor characterization.

Dr. Chu is a member of the Acoustical Society of America.